Kinetic Study of Alizarin Saphirol and Indigo Carmine Dyes Adsorption Process

ALEXANDRA RALUCA MIRON[1]*, ABBAS ABDUL KADHIM KLAIF RIKABI[1,2], ALEXANDRA-GABRIELA NICULAE[1], SZIDONIA-KATALIN TANCZOS[1,3]

[1]University Politehnica of Bucharest, Analytical Chemistry and Environmental Engineering Department, 1-7 Ghe. Polizu Str., 011061, Bucharest, Romania

[2] Foundation of Technical Education, Baghdad, Iraq

[3] Sapientia University, 1 Libertatii Sq., 530104, Miercurea Ciuc, Romania

Electrocoagulation is an electrochemical method based on the in situ generation of coagulating agents by sacrifical anodes use. In this paper we aimed to study the adsorption process kinetics of two dyes with multiple industrial uses, namely, Indigo Carmine and Alizarin Saphirol. Also, the influence of current density and initial pH value on adsorption process kinetics was evaluated. The results revealed that on aluminum anodes, the highest adsorption process rates and the lowest half – time values were obtained at pH = 6. In the case of iron anodes use, we have noticed that the half-time decreased with increasing pH and the initial adsorption rate values increase with pH increasing.

Keywords: adsorption, electrocoagulation, dyes removal, kinetic modelling

It is generally considered that the pollutant removal when using electrocoagulation is due to its adsorption on the surface of flocs generated inside the electrochemical cell under the direct influence of the applied current density [1,2].

In a complex process, the process speed is determined by the slowest step. Critical analysis of dye solutions electrocoagulation showed the existence of two separate processes occurring in the electrochemical cell [3,4,17], namely:

- the electrochemical process itself which generates flocs;
- the physico-chemical process in which the pollutant is adsorbed on the surface of the flocs formed in the previous step [5,6].

Because the electrochemical process speed is much higher than the one of the physico-chemical process, it is considered that the process underlying the pollutant elimination is similar to classical adsorption, except for the step of floc generation, fact which highlights the importance and need of a study regarding the *in situ* generated flocs adsorption ability of the dyes studied [10-12,19].

By means of kinetic study regarding the Indigo Carmine and Alizarin Safirol dyes adsorption on the flocs electrochemically generated inside the electrocoagulation cell we aimed to establish the pollutants adsorbtion speed.

Since we can estimate the amount of coagulant agent generated in the system at time t, the electrocoagulation system behavior used to remove dyes can be modeled using adsorption processes[7, 9, 15].

During the electrocoagulation process, the insoluble metal hydroxides contribute to the removal of colorants through surface adsorption.

During the adsorption process is presumed that the pollutant acts as a ligand binding to the Al/Fe hydroxides formed in the electrocoagulation cell with the formation of a gelatinous precipitate [13,15].

$$\frac{dq_t}{dt} = k(q_e - q_t)^2 \quad (1)$$

For the interpretation of the experimental results obtained from the electrocoagulation studies we used a kinetic model of pseudo-second order. Using this model, we've been also calculated the kinetic parameters of the two dyes selected for the study adsorption process. The reactions below describe the second order kinetics that we have used [5,14].

Where q_e is the amount of dye absorbed at equilibrium, q_t represents the amount of dye adsorbed at time t, and k is the pseudo-second order kinetic constant.

By integrating the above equation taking into account the boundary conditions t = 0- t q_t = 0 - q_t the following formula is obtained [5,18]:

$$\frac{1}{(q_e - q_t)} = \frac{1}{q_e + kt} \quad (2)$$

Rearranging the terms, the linearized form of equation is obtained:

$$\frac{t}{q_t} = \frac{1}{k_2 \cdot q_e^2} + \frac{1}{q_e} t \quad (3)$$

$$v_0 = k \cdot q_e^2 \quad (4)$$

$$t_{1/2} = \frac{1}{k \cdot q_e} \quad (5)$$

where: v_0 is the initial dye adsorption process speed, mg / g min and $t_1/_2$ is the half-life, min.

From the graphical representation of the t/q_t parameter versus electrocoagulation time it can be determined the pseudo-second order rate constant, k [20,5]

Experimental part

Materials and methods

Alizarin Saphirol and Indigo Carmin dye were provided by Sigma-Aldrich and used as received without further purification. All chemicals used in this study were of analytical grade [8].

* *email: andra3005@yahoo.com*

Experimental procedure description

The dyes solutions were prepared by dissolving a required quantity of Alizarin Saphirol, respectively Indigo Carmine dye powder in distillated water in order to reduce the interferences. At the begining of the each run, 1000 mL of solution was prepared and 800 mL were placed in the electrochemical cell, the electrodes were immersed in solution and connected to a Mastech HY3005D DC power supply.

The *p*H of the aqueous samples was adjusted to desired value using 6% H_2SO_4 and respectively, 0.1N NaOH solutions and during the whole period of experiments was monitored using a Consort C380 pH-meter (0.01 *p*H resolution, Pt1000 sensor).

At the end of the electrocoagulation experiments, before analysis, the samples were filtered using white ribbon filter paper. The dye concentration was determined at the wavelenght corresponding to the maximum absorbance (600 nm for Alizarin Saphirol, respectively 610 nm for Indigo Carmine) using a UV-Vis double beam spectrophotometer Cintra 5 (spectral range 190-1100 nm) [16].

Results and discussions

The solution pH influence

From the graphical representation of Alizarin Saphirol dye adsorption capacity varriation in time (fig. 1a) it can be observed that the process is fast both in the case of aluminum and iron anodes, reaching equilibrium after about 3 min in the case of iron respectively 8 min in the case of aluminum electrodes.

We also noted that is the case of aluminum anodes, the highest load levels were obtained at *p*H = 6, fact which is consistent with the very good results obtained previously for the colour removal degree at the same amount of working solution *p*H.

A possible explanation for this system behaviour can be correlated with the fact that at *p*H = 6 in the system predominates some aluminum complex having great capacity for adsorption of dye molecules.

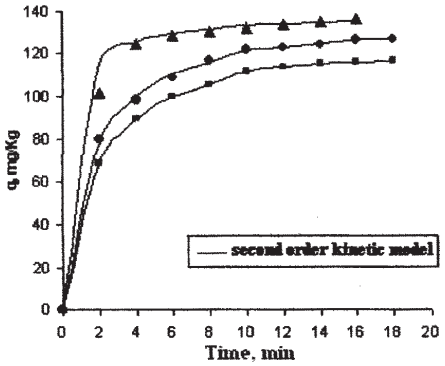

Fig. 1a. Alizarin Saphirol adsorption process kinetic, $C_i = 5 \cdot 10^{-5}$ M, working pH values: 4 (•), 6 (▲), 10(▪), Al anodes

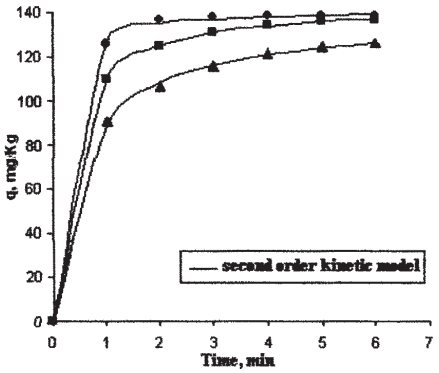

Fig.1b. Alizarin Saphirol adsorption process kinetic, $C_i = 5 \cdot 10^{-5}$ M, working pH values: 2 (•),6 (▲),8 (▪), Fe anodes

Regarding the results that we have obtained with iron anodes (fig. 1b), it is obvious that after only two minutes of electrocoagulation, in the system, at *p*H = 8, there are enough active species capable of adsorbing a significant amount of dye .

In figure 1c are presented the results that we have obtained in the study of working solution *p*H influence on the adsorption process kinetic and thus, on the adsorption capacity.

On the basis of the data obtained for aluminum anodes at an initial concentration of $1\ 10^{-4}$ M, it can be seen that the adsorption capacity value increases from 9.47 mg/kg recorded at *p*H = 10 to 20.49 mg/kg at *p*H = 6. For a $5\ 10^{-4}$ M inital concentration, the adsorption capacity of the metal hydroxide flocs is growing from 55.03 mg/kg at *p*H = 10, to 127.51 mg/kg to *p*H = 6.

The adsorption capacity of the iron hydroxides (fig. 1d) for an initial Alizarin Saphirol solution concentration of $1\ 10^{-4}$ M is about 22.13 mg dye/kg metal hydroxide at a working solution *p*H value = 2, while at *p*H = 8 is of 42.91 mgdye/ kg metal hydroxide.

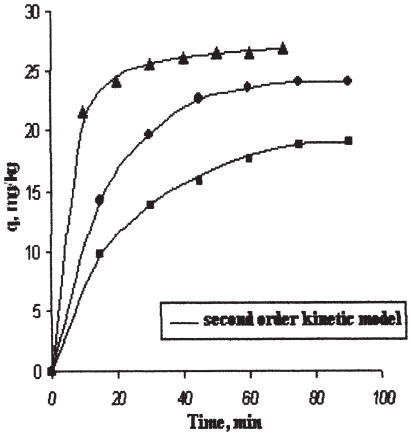

Fig. 1c.Alizarin Saphirol adsorption process kinetic, $C_i = 1 \cdot 10^{-4}$ M, working pH values: 4 (•),6 (▲),10(▪), Al anodes

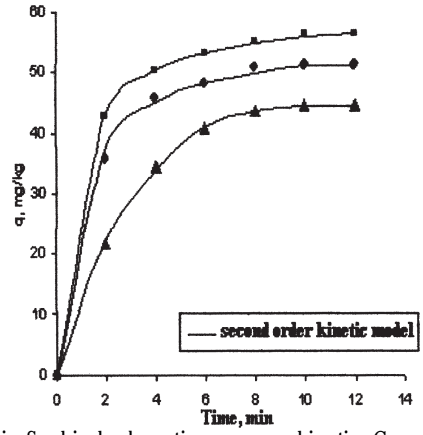

Fig. 1d. Alizarin Saphirol adsorption process kinetic, $C_i = 1 \cdot 10^{-4}$ M, working pH values: 2 (•), 6 (▲),8 (▪), Fe anodes

The results obtained for an initial working solution concentration of $5\ 10^{-4}$ M (fig. 2a and 2b,) reveals that the largest adsorption capacity was obtained at *p*H = 8, and the lowest at *p*H = 2, which is in agreement with the prevoius results obtained for colour removal efficiency.

In figures 2c, 2d -3 we presented the experimental results obtained for the study of inital *p*H value influence on the adsorption process kinetic of Indigo Carmine dye.

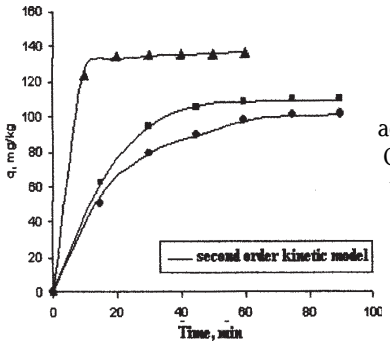

Fig.2a. Alizarin Saphirol adsorption process kinetic, $C_i = 5 \cdot 10^{-4}$ M, working *p*H values: 4(•),6 (▲),10(▪), Al anodes

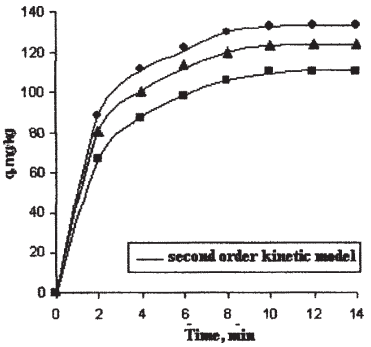

Fig. 2b. Alizarin Saphirol adsorption process kinetic, $C_i = 1 \cdot 10^{-4}$ M, working *p*H values: 2 (•), 6 (▲),8 (▪), Fe anodes

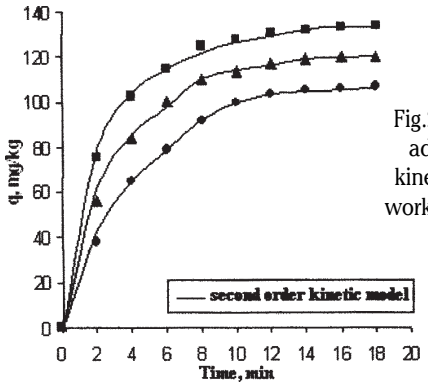

Fig.2c. Indigo Carmine adsorption process kinetic, $C_i = 5 \cdot 10^{-5}$ M, working *p*H values: 4(•), 6 (▲), 10 (▪), Al anodes

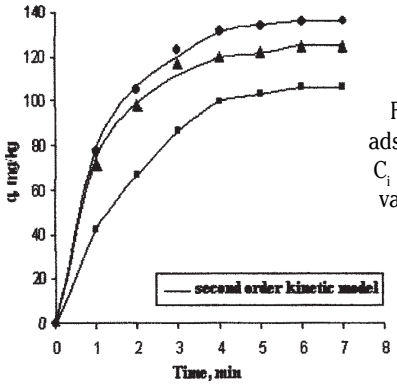

Fig.2d. Indigo Carmine adsorption process kinetic, $C_i = 5 \cdot 10^{-5}$ M, working *p*H values: 2 (•), 6 (▲),8 (▪), Fe anodes

Unlike Alizarin Saphirol, we've been noted that the adsorption process is slower, the time required for reaching the equilibrium being higher and significantly inffluenced by the dye solution initial concentration, namely the anode material type chosen for the studies.

Thus, in the case of aluminum anodes at an initial Indigo Carmine concentration of $5\ 10^{-4}$ M, the adsorption capacity increases from 140.56 mg dye/kg metal hydroxide at *p*H = 10, to 201.56 mg dye/kg metal hydroxide at *p*H = 6, while for at a $5\ 10^{-5}$ M concentration, the adsorption capacity increases from 42.43 mg dye / kg metal hydroxide at *p*H = 10, to 79.18 mg dye / kg metal hydroxide at *p*H = 6.

Regarding the results obtained for the kinetic studies done on iron sacrificial anodes, we have noticed that the *p*H value influences the adsorption capacity, because for the same Indigo Carmine solution concentration we have noted an increase in the adsorption capacity with increasing the *p*H of the solution.

Thus, the adsorption capacity increases from at an initial concentration of $5\ 10^{-5}$ M from 42.14 mg/ kg at *p*H = 2 to 79.56 mg / kg at *p*H = 8, while at a concentration of $5\ 10^{-4}$ M, the capacity is increased from 185.17 mg / kg at *p*H = 2 at 212.77 mg / kg at *p*H = 8.

In figures 4a and 4b we revealed the graphical representation of the second order kinetic equation linearized form for Alizarin Saphirol - aluminum, respectively iron anodes system.

From the data analysis we have seen that the correlation coefficients values for the processed data sets are very close to 1, which suggests that the adsorption is indeed described by a pseudo - second order kinetic.

The relevant parameters obtained using the second order kinetic equation are shown in tables 1-4.

With the regard to the kinetic parameters specific for the adsorption process, namely, the initial speed and half-life, their values are influenced by the initial *p*H.

Thus, in the case of Alizarin Saphirol, on aluminum anodes, the highest adsorption process rates values and the lowest half time values were obtained at *p*H = 6.

For the experiments realised using iron sacrificial anodes we've noticed that the half-time decreases with increasing the *p*H, whereas the initial adsorption rate values increase with *p*H increase.

A similar system behavior was observed for Indigo Carmine.

From the graphical representation of the kinetic equation linearized form shown in figure 4c and figure 4d we observed that the experimental data obtained for Indigo Carmine dye fits well on the theoretical curves obtained from the pseudo-second order kinetic model, for both experiments carried out on aluminum and respectively iron anodes.

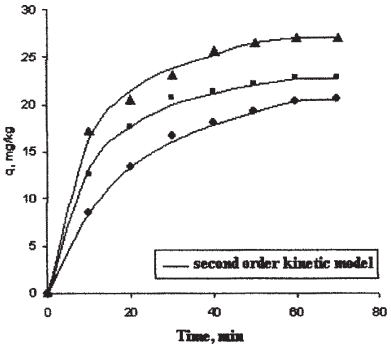

Fig.3a. Indigo Carmine adsorption process kinetic, $C_i = 1 \cdot 10^{-4}$ M, working pH values: 4(•), 6 (▲), 10 (▪), Al anodes

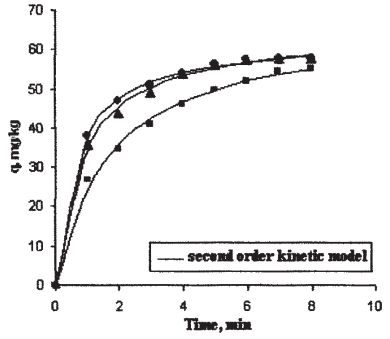

Fig.3b. Indigo Carmine adsorption process kinetic, $C_i = 1 \cdot 10^{-4}$ M, working pH values: 2 (•), 6 (▲), 8 (▪), Fe anodes

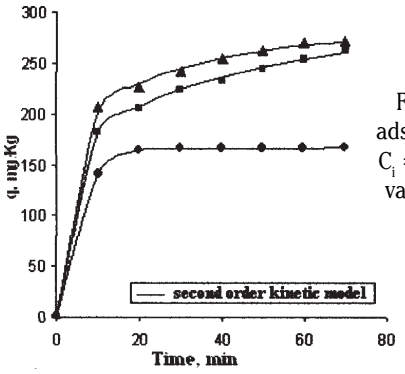

Fig. 3c. Indigo Carmine adsorption process kinetic, $C_i = 5 . 10^{-4}$ M, working pH values: 4(•),6 (▲), 10 (▪), Al anodes

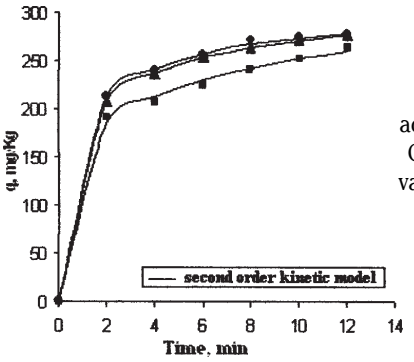

Fig. 3d Indigo Carmine adsorption process kinetic, $C_i = 5 .10^{-4}$ M, working pH values s: 2 (•), 6 (▲), 8 (▪), Fe anodes

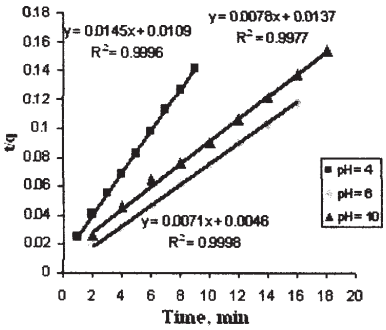

Fig. 4a. Graphical representation of the second order kinetic equation linearized form for Alizarin Saphirol - aluminum anodes system

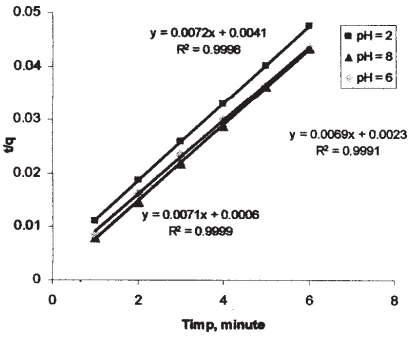

Fig. 4b. Graphical representation of the second order kinetic equation linearized form for Alizarin Saphirol - iron anodes system

	Alizarin Saphirol initial concentration, M											
pH	$5 \cdot 10^{-5}$				$1 \cdot 10^{-4}$				$5 \cdot 10^{-4}$			
	k	$t_{1/2}$	q_e	v_0	k	$t_{1/2}$	q_e	v_0	k	$t_{1/2}$	q_e	v_0
4	0.004	1.498	137.911	92.011	0.007	4.221	32.666	7.737	0.0009	20.370	54.295	2.665
6	0.018	0.397	138.254	348.234	0.017	1.899	30.711	16.164	0.008	0.844	138.282	163.810
10	0.004	1.759	128.749	73.188	0.006	4.361	37.524	8.603	0.0004	19.286	125.787	6.522

Table 1
VALUES OF SECOND-ORDER KINETIC EQUATION PARAMETERS FOR ALIZARIN SAPHIROL-ALUMINIUM ANODES SYSTEM

	Alizarin Saphirol initial concentration, M											
pH	$5 \cdot 10^{-5}$				$1 \cdot 10^{-4}$				$5 \cdot 10^{-4}$			
	k	$t_{1/2}$	q_e	v_0	k	$t_{1/2}$	q_e	v_0	k	$t_{1/2}$	q_e	v_0
2	0.012	0.563	138.213	245.489	0.006	2.679	56.245	20.991	0.004	1.846	128.501	69.594
6	0.021	0.321	144.574	450.150	0.018	0.987	55.939	56.647	0.004	1.480	140.311	94.804
8	0.078	0.090	140.910	1550.564	0.020	0.814	60.397	74.128	0.004	1.393	150.006	107.619

Table 2
VALUES OF SECOND-ORDER KINETIC EQUATION PARAMETERS FOR ALIZARIN SAPHIROL-IRON ANODES SYSTEM

	Indigo carmine initial concentration, M											
pH	$5 \cdot 10^{-5}$				$1 \cdot 10^{-4}$				$5 \cdot 10^{-4}$			
	k	$t_{1/2}$	q_e	v_0	k	$t_{1/2}$	q_e	v_0	k	$t_{1/2}$	q_e	v_0
4	0.002	2.571	139.835	54.377	0.003	9.834	26.350	2.679	0.009	3.6893	27.680	7.502
6	0.003	1.729	147.649	85.392	0.003	8.824	30.715	3.480	0.0003	16.424	161.082	9.807
10	0.001	4.452	136.889	30.746	0.001	20.224	26.857	1.327	0.0001	35.072	179.815	5.126

Table 3
VALUES OF SECOND-ORDER KINETIC EQUATION PARAMETERS FOR INDIGO CARMINE-ALUMINIUM ANODES SYSTEM

	Indigo carmine initial concentration, M											
pH	$5 \cdot 10^{-5}$				$1 \cdot 10^{-4}$				$5 \cdot 10^{-4}$			
	k	$t_{1/2}$	q_e	v_0	k	$t_{1/2}$	q_e	v_0	k	$t_{1/2}$	q_e	v_0
2	0.002	2.821	161.086	57.083	0.008	1.747	67.002	38.332	0.0009	6.102	180.535	29.584
6	0.007	0.940	145.825	155.115	0.017	0.874	64.880	74.205	0.0018	3.190	172.781	54.151
8	0.006	1.023	160,.954	157.333	0.023	0.681	63.162	92.662	0.0021	2.700	169.632	62.804

Table 4
VALUES OF SECOND-ORDER KINETIC EQUATION PARAMETERS FOR INDIGO CARMINE-IRON ANODES SYSTEM

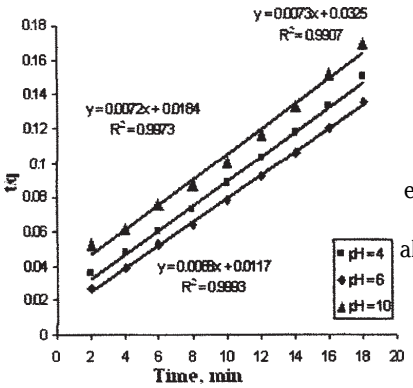

Fig. 4c. Graphical representation of the second order kinetic equation linearized form for Indigo Carmine - aluminum anodes system

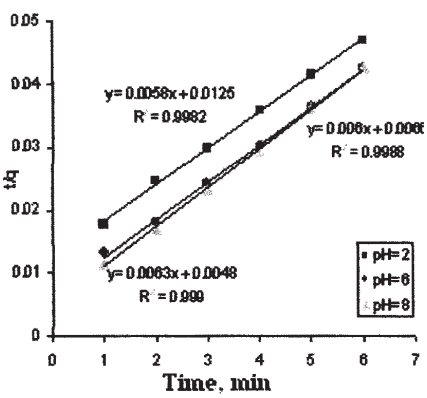

Fig. 4d. Graphical representation of the second order kinetic equation linearized form for Indigo Carmine - iron anodes system

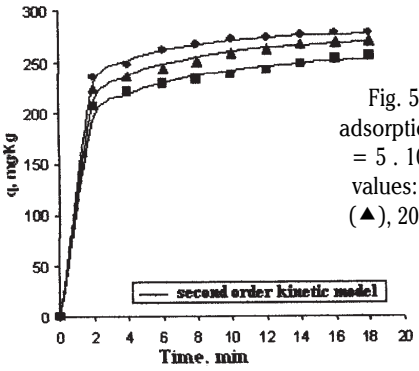

Fig. 5a. Alizarin Saphirol adsorption process kinetic, C_i = 5 . 10^{-5} M, current density values: 50 A/m^2 (•),100 A/m^2 (▲), 200 A/m^2 (▪), Al anodes

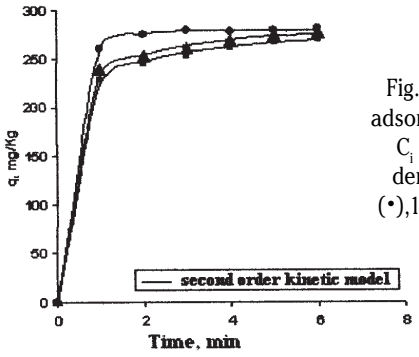

Fig. 5b. Alizarin Saphirol adsorption process kinetic, C_i = 5 . 10^{-5} M, current density values: 50 A/m^2 (•),100 A/m^2 (▲), 200 A/m^2 (▪),Fe anodes

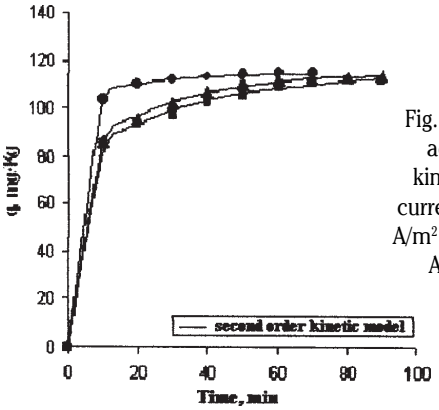

Fig. 5c. Alizarin Saphirol adsorption process kinetic, C_i = 1 . 10^{-4} M, current density values: 50 A/m^2 (•), 100 A/m^2 (▲), 200 A/m^2 (▪), Al anodes

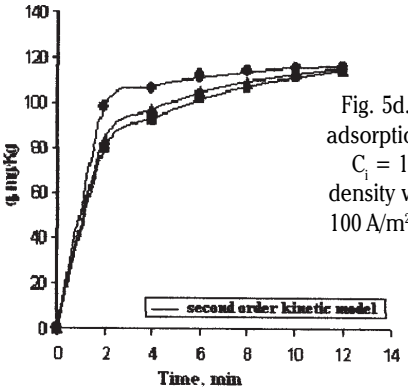

Fig. 5d. Alizarin Saphirol adsorption process kinetic, C_i = 1 . 10^{-4} M, current density values: 50 A/m^2 (•), 100 A/m^2 (▲), 200 A/m^2 (▪), Fe anodes

Current density inffluence

In figures 5a and 5b are presented the experimental results that have been obtained with regard to the Alizarin Saphirol dye adsorption on the flocs generated in the system process kinetic with highlighting the effect of current density on the the adsorption process efficiency.

From figure 5a we have noted that on aluminum anodes, at an initial solution concentration of 5 10^{-5}M, the adsorption process is slower, the adsorption equilibrium being reached after approximately 10-12 min, while on iron anode the adsorption equilibrium is reached after 4 min (fig. 5b).

We have also noticed that the current density value influences the adsorption capacity of flocs, thus, for the same Alizarin Saphirol initial concentration an increase in the adsorption capacity with current density increasing was recorded.

From the analysis of data obtained for aluminum anodes (fig. 5c) at an initial concentration of 1 10^{-4} M, it was observed that the adsorption capacity increased from 82.44 mg / kg at 50 A/m^2 to 103.37 mg / kg at i = 200 A/m^2 while for an initial concentration of 5 10^{-4} M, the metal hydroxide flocs adsorption capacity increased from 184.56 mg/kg at a 50 A/m^2 current density to 209 407 mg / kg for i = 200 A/m^2.

Regarding the results obtained for the adsorption capacity evolution when using iron anodes (fig. 5d), at an initial 1 10^{-4} M concentration of Alizarin Saphirol solution it is about 80.29 mg dye / kg metal hydroxide, at a current density of 50 A/m^2, while at 200 A/m^2, is 98.11 mg dye/kg metal hydroxide.

The results obtained for a 5 10^{-4} M initial solution concentration (fig. 6a and fig. 6b) reveal that the highest

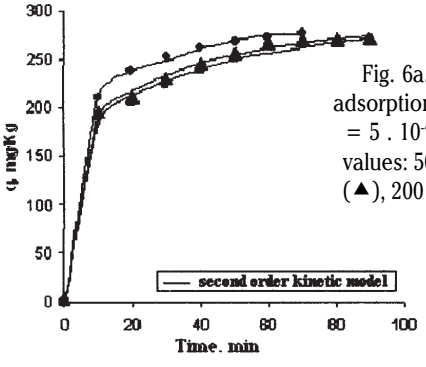

Fig. 6a. Alizarin Saphirol adsorption process kinetic, C_i = 5 . 10^{-4} M, current density values: 50 A/m^2 (•), 100 A/m^2 (▲), 200 A/m^2 (▪), Al anodes

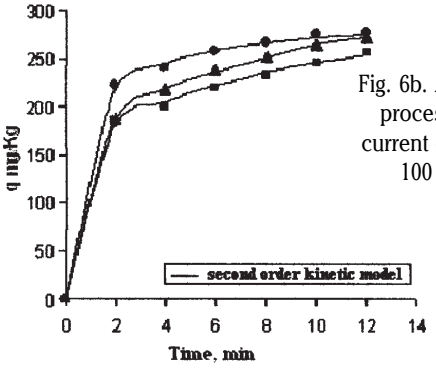

Fig. 6b. Alizarin Saphirol adsorption process kinetic, C_i = 1 . 10^{-4} M, current density values: 50 A/m^2 (•), 100 A/m^2 (▲), 200 A/m^2 (▪), Fe anodes

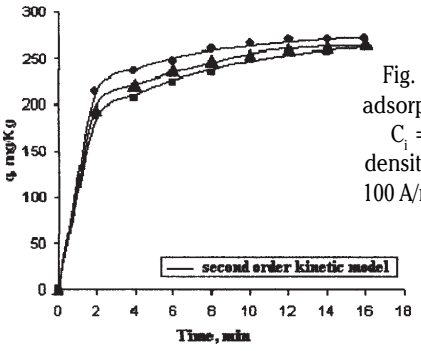

Fig. 7a. Indigo Carmine adsorption process kinetic, C_i = 5. 10^{-5} M, current density values: 50 A/m^2 (•), 100 A/m^2 (▲), 200 A/m^2(▪), Al anodes

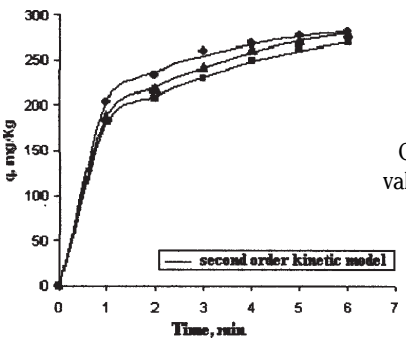

Fig. 7b. Indigo Carmine adsorption process kinetic, C_i = 5 . 10^{-5} M, current density values: 50 A/m^2 (•), 100 A/m^2 (▲), 200 A/m^2 (▪), Fe anodes

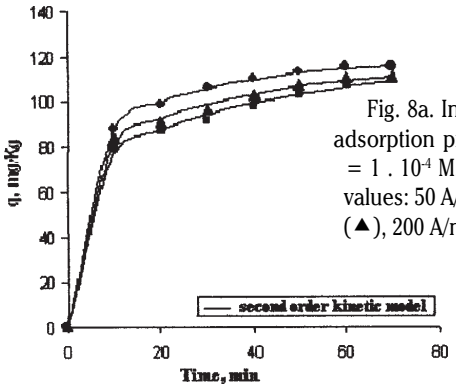

Fig. 8a. Indigo Carmine adsorption process kinetic, C_i = 1 . 10^{-4} M, current density values: 50 A/m^2 (•), 100 A/m^2 (▲), 200 A/m^2 (▪), Al anodes

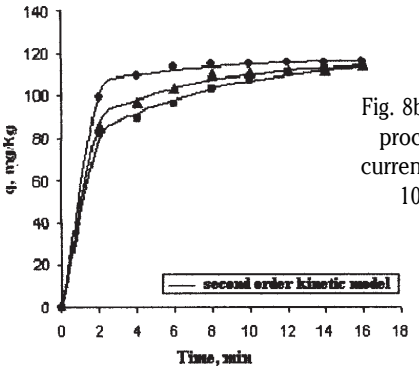

Fig. 8b. Indigo Carmine adsorption process kinetic, C_i = 1 . 10^{-4} M, current density values: 50 A/m^2 (•), 100 A/m^2 (▲), 200 A/m^2 (▪), Fe anodes

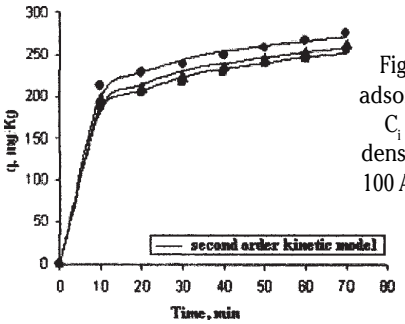

Fig. 9a. Indigo Carmine adsorption process kinetic, C_i = 5 . 10^{-4} M, current density values: 50 A/m^2 (•), 100 A/m^2 (▲), 200 A/m^2 (▪), Al anodes

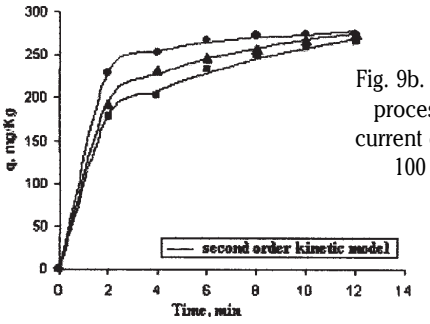

Fig. 9b. Indigo Carmine adsorption process kinetic, C_i = 5 . 10^{-4} M, current density values: 50 A/m^2 (•), 100 A/m^2 (▲), 200 A/m^2 (▪), Fe anodes

adsorption capacity value was obtained at i = 200 A/m^2 and the lowest at i = 50 A/m^2, which is consistent with the results obtained previously for colour removal efficiency.

In figures 7-9 we presented the experiment results conducted for the study of initial current density value influence on the Indigo Carmine dye adsorption kinetics.

As in the case of Alizarin Saphirol, the current density value applied to the cell affects the adsorption capacity of the flocs generated in the electrochemical cell. Also, it can be seen that the time necessary to achieve adsorption equilibrium is determined by the initial dye solution concentration and by the anode material type.

For example, in the case of aluminum anodes (fig. 7a), at an initial Indigo Carmine concentration of 5 10^{-5} M, the adsorption capacity increases from 183.73 mg dye / kg metal hydroxide at i = 50 A/m^2 to 211.76 mg dye / kg metal hydroxide at i = 200 A/m^2, while for an initial concentration of 5 10^{-4} M (fig. 9a), the adsorption capacity increases from 182.61 mg dye / kg metal hydroxide at i = 50 A/m^2 to 201.18 mg dye / kg metal hydroxide at i = 200 A/m^2.

From the analysis of the results obtained from the kinetic studies performed on sacrificial anodes made of iron, we have seen that increasing current density value leads to an increase of the adsorption capacity.

Thus, the adsorption capacity increases at an initial concentration of 5 10^{-5} M (fig. 7b) from 180.91 mg/kg at i = 50 A/m^2 to 204.25 mg / kg at a 200 A/m^{2}current density, while at a concentration of 5 10^{-4} M (fig. 9b) the capacity increases from 179.53 mg/kg at i = 50 A/m^2, up to 212.77 mg/kg at i = 200 A/m^2.

The relevant parameters obtained using the second order kinetic equation are shown in tables 5-9.

i, A/m^2	Alizarin Saphirol initial concentration, M											
	$5\cdot10^{-5}$				$1\cdot10^{-4}$				$5\cdot10^{-4}$			
	k	$t_{1/2}$	q_e	v_0	k	$t_{1/2}$	q_e	v_0	k	$t_{1/2}$	q_e	v_0
50	0.003	2.544	127.512	50.104	0.0009	16.474	63.631	3.862	0.0001	29.416	173.255	5.889
100	0.003	2.011	143.339	71.254	0.001	13.448	64.108	4.767	0.0002	24.746	170.505	6.889
200	0.005	1.315	147.625	112.202	0.005	3.134	59.054	18.840	0.0004	13.550	162.024	11.957

Table 5
VALUES OF SECOND-ORDER KINETIC EQUATION PARAMETERS FOR ALIZARIN SAPHIROL-ALUMINIUM ANODES SYSTEM

i, A/m^2	Alizarin Saphirol initial concentration, M											
	$5\cdot10^{-5}$				$1\cdot10^{-4}$				$5\cdot10^{-4}$			
	k	$t_{1/2}$	q_e	v_0	k	$t_{1/2}$	q_e	v_0	k	$t_{1/2}$	q_e	v_0
50	0.009	0.741	145.351	196.121	0.002	5.561	82.736	14.876	0.0007	7.209	180.511	25.037
100	0.011	0.607	148.673	244.832	0.003	3.794	75.212	19.820	0.0007	6.853	207.741	30.311
200	0.042	0.162	143.391	880.87	0.013	1.204	63.601	52.820	0.002	2.166	160.672	74.173

Table 6
VALUES OF SECOND-ORDER KINETIC EQUATION PARAMETERS FOR ALIZARIN SAPHIROL-IRON ANODES SYSTEM

i, A/m^2	Indigo carmine initial concentration, M											
	$5\cdot10^{-5}$				$1\cdot10^{-4}$				$5\cdot10^{-4}$			
	k	$t_{1/2}$	q_e	v_0	k	$t_{1/2}$	q_e	v_0	k	$t_{1/2}$	q_e	v_0
50	0.001	5.618	164.296	29.240	0.002	4.827	72.656	15.049	0.0002	26.022	151.305	5.814
100	0.001	3.691	153.892	41.689	0.005	2.619	65.386	24.959	0.0002	22.654	154.708	6.828
200	0.003	2.211	149.842	67.762	0.020	0.805	61.167	75.976	0.0003	16.127	158.285	9.814

Table 7
VALUES OF SECOND-ORDER KINETIC EQUATION PARAMETERS FOR INDIGO CARMINE-ALUMINIUM ANODES SYSTEM

i, A/m^2	Indigo carmine initial concentration, M											
	$5\cdot10^{-5}$				$1\cdot10^{-4}$				$5\cdot10^{-4}$			
	k	$t_{1/2}$	q_e	v_0	k	$t_{1/2}$	q_e	v_0	k	$t_{1/2}$	q_e	v_0
50	0.0008	4.851	235.879	48.617	0.002	4.827	72.656	15.049	0.0001	29.416	173.255	5.889
100	0.001	4.016	236.101	59.000	0.005	2.619	65.386	24.959	0.0002	24.746	170.505	6.889
200	0.002	1.990	190.306	95.625	0.020	0.805	61.167	75.976	0.0004	13.550	162.024	11.957

Table 8
VALUES OF SECOND-ORDER KINETIC EQUATION PARAMETERS FOR INDIGO CARMINE-IRON ANODES SYSTEM

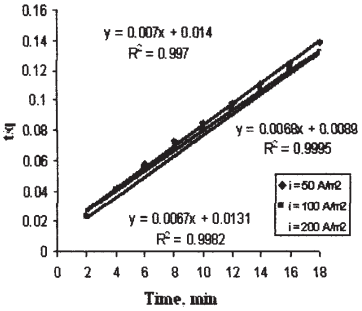

Fig. 10a. Graphical representation of the second order kinetic equation linearized form for Alizarin Saphirol - aluminum anodes system

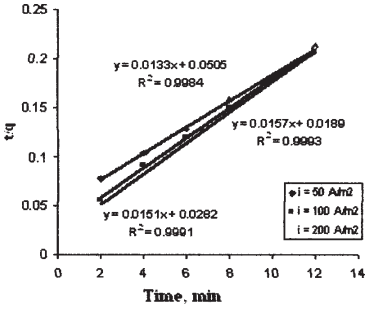

Fig. 10b. Graphical representation of the second order kinetic equation linearized form for Alizarin Saphirol - iron anodes system

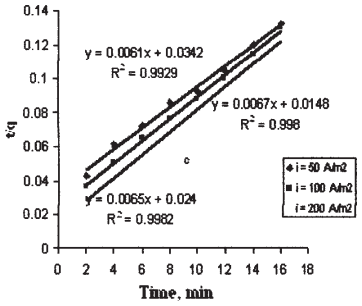

Fig. 11a. Graphical representation of the second order kinetic equation linearized form for Indigo Carmine - aluminum anodes system

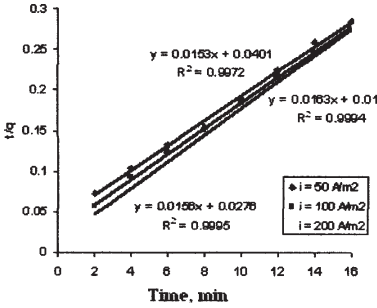

Fig. 11b Graphical representation of the second order kinetic equation linearized form for Indigo Carmine - iron anodes system

With regard to the specific kinetic parameters of the adsorption process, namely the initial speed and half-time, their values are influenced by the current density at which the experiments are done.

Thus, both in the case of Alizarin Saphirol and Indigo Carmine the results obtained on aluminum, respectively, iron anodes indicates that the initial rate of adsorption increases by increasing the current density value while the half-time is reduced when current density is increased.

In figures 10a and 10b, we presented the graphical representation of linearized form of the second order kinetic equation in the case of Alizarin Saphirol – aluminum/iron anodes system.

From the analysis results we have seen that the correlation coefficients values for the processed data sets are very close to 1, which suggests that indeed the adsorption process follows a pseudo - second order kinetics.

From the graphical representation of the kinetic equation linearized form shown in figures 11a and 11b we observed that the experimental obtained for Indigo Carmine dye fall well on the theoretical curves obtained from the pseudo-second order kinetic model, both for experiments carried out on aluminum and iron anodes.

Conclusions

Because the speed of the electrochemical process is much higher than the physicochemical process, it is considered that the underlying pollutant elimination is similar to classical adsorption, except for the step of flocs generation, which highlights the importance and need for a study on the ability of dyes adsorption on the *in situ* generated flocs.

By realising a kinetic study for the adsorption of Indigo Carmine and Alizarin Saphirol dyes on the flocs electrochemically generated inside the electrocoagulation cell, we aimed to establish the pollutants adsorbtion rate in different working conditions.

The results revealed that on aluminum anodes, the highest adsorption process rates and the lowest half – time values were obtained at *p*H = 6.

In the case of iron anodes use, we have noticed that the half-time decreased with increasing *p*H and the initial adsorption rate values increase with *p*H increasing.

Also, based on the graphical representation the kinetic equation linearized form we have noted that the experimental data obtained for the two dyes studied can be described mathematically precise enough with pseudo-second order kinetic model for both experiments done on aluminum and iron anodes, which demonstrates that the adsorption of these compounds follows a second order kinetic.

Acknowledgements: The work has been funded by the Sectoral Operational Programme Human Resources Development 2007-2013 of the Ministry of European Funds through the Financial Agreement POSDRU/159/1.5/S/134398.

References

1.BALASUBRAMANIAN, N., KOJIMA, T., SRINIVASAKANNAN, C., Chem. Eng. J., **155,** 2009, p.76–82
2.ALVARES, A.B.C., DIAPER, C., PARSONS, S.A., Environ. Technol., **22**, 2001, p.409-427
3.CARLETTO, R.A., CHIMIRRI, F., BOSCO, F., FERRERO, F., BioResources, **4**, 2008, p.1146-1155.
4.DANESHVAR, N., OLADEGARAGOZE, A., DJAFARZADEH, N., J. Haz. Mat., **B 129,** 2006, 116–122
5.CHITHRA, K., BALASUBRAMANIAN, N., JMSS, **1,** 2010, p.124-130
6.ESSADKI, A.H., BENNAJAH, M., GOURICH, B., VIAL, CH., AZZI, M., DELMAS, H., Chem. Eng. Process, **47**, 2008, p.1211–1223
7.SENTHILKUMAR, P., UMAIYAMBIKA, N., GAYATHRI, R., Environm. Eng Manag. J ,**9**, 2010, p.1031-1037
8.MIRON, A. R., MODROGAN C., ORBULEŢ O. D., Rev. Chim.(Bucharest), **61**, no. 7, 2010, p.646
9.CHOU, W.L., WANG, C.T., HUANG, K.Y., J. Haz. Mat., **167,** 2009, p.467–474
10.DANESHVAR N., SORKHABI ASHASSI, H., KASIRI, M.B., J. Haz. Mat., **B112**, 2004, p.55–62
11.CHOU, W.L., WANG, C.T., HUANG, K.Y., Desal., **251**, 2010, P.12-19
12.MOUEDHEN, G., FEKI, M., DE PETRIS WERY, M., AYEDI, H.F., J.Haz.Mat., **150**, 2008, p.124-135
13.ZHANG, X.D., HAO, J.D., LI, W.S., JIN, H.J., YANG, J., HUANG, Q.M. , LU, D.S. , XU, H.K., J.Haz.Mat., **170**, 2009, p.883-887
14.SASSON, M. B., CALMANO, W., ADIN, A., J.Haz.Mat., **171**, 2009, p.704-709
15.BEHNAJADY, M.A., MODIRSHAHLA N., SHOKRI M., VAHID B., J.Haz.Mat., **165**, 2009, p.168-173
16.MIRON, A. R., ORBULEŢ, O., MODROGAN, C., Rev. Chim.(Bucharest), **62**, no. 2, 2011, p. 163
17.MOHEY EL-DEIN, A., LIBRA, J.A., WIESMANN, U., Chemosphere, **52**, 2003, p.1069–1077
18.TSAI, W.T., CHANG, C.Y., ING, C.H., CHANG, C.F., JCIS, **275**, 2004, p.72-78
19.DURANGO-USUGA, P., GUZMÁN-DUQUE, F., MOSTEO, R., VAZQUEZ, M. V., PNUELA, G., TORRES-PALMA, R. A., J.Haz.Mat., 179, 2010, p.120-126
20.TROMPETTE, J.L., VERGNES, H., J.Haz.. Mat. **163**, 2009 ,p. 1282–1288

Manuscript received: 15.07.2014